Check for updates

RESEARCH ARTICLE

Macromolecular Rapid Communications
www.mrc-journal.de

A Polymer Acceptor with Grafted Small Molecule Acceptor Unit for Efficient All Polymer Organic Solar Cells

Wendi Shi, Yuzhong Huang, Kangqiao Ma, Xiaodong Si, Wanying Feng, Ruohan Wang, Jiaxin Guo, Wei Ma, Shijie Wang, Andrew Clulow, Lester Barnsley, Zhaoyang Yao, Chenxi Li,* Xiangjian Wan,* and Yongsheng Chen*

A polymer acceptor, named PX-1, is designed and synthesized using a polymerization strategy with grafted small molecule acceptors. This design approach allows for the freedom of end groups while maintaining efficient terminal packing, enhancing π–π interactions, and facilitating charge transport. All-polymer organic solar cells based on PM6: PX-1 demonstrate a promising efficiency of 13.55%. The result presents an alternative pathway for the design of high-efficiency polymer acceptors through the careful regulation of small molecule acceptor monomers and linker units.

1. Introduction

In recent decades, organic solar cells (OSCs) have drawn significant attention due to their remarkable advantages, including lightweight nature, semitransparency, and solution processability, etc.[1–3] Through extensive research in molecular design and device optimization,[4–12] single-junction OSCs based on polymer donors and small molecule acceptors (SMAs) have achieved impressive power conversion efficiency (PCE) surpassing 19%.[13–15] While polymer/SMAs-based OSCs have made significant progress, all-polymer solar cells (all-PSCs) have emerged as a promising alternative. All-PSCs utilize polymer donors and polymer acceptors in the photoactive layers, offering distinct advantages such as excellent thermal and morphological stability, remarkable stretchability, and mechanical durability.[16–19] Despite the progress made in all-PSCs, with PCEs exceeding 18% [20–23] due to the development of "polymerized small-molecule acceptors" (PSMAs),[24,25] they still fall behind the performance of SMAs-based OSCs. This disparity can be attributed to the limited availability of high-performance polymer acceptors and the challenges associated with regulating the blend morphology in all-polymer systems. To address these issues, further advancements in the development of new PSMAs are essential.

Currently, there have been numerous reports on high-performance PSMAs achieved by directly polymerizing Y-series SMAs with different linkers.[21,26,27] However, most polymer acceptors are copolymerized through terminal units and linkers, which comes with certain disadvantages that cannot be ignored. First, it affected intermolecular packing. The intermolecular packing facilitated by electron-deficient terminal groups has been recognized as an effective packing mode in non-fullerene SMAs, as supported by a considerable number of single-crystal structures.[28,29] This packing mode establishes efficient charge transfer channels, thereby improving short-circuit current density (J_{SC}) and fill factor (FF). However, when terminal units of SMAs are utilized for polymerization with other linkers, the electron-deficient nature of terminal groups and the original packing mode of SMAs are significantly altered. Moreover, studies have demonstrated that the planarity of PSMAs' skeleton can be affected by the torsion angle between the bridging unit and the terminal group,[18,30,31] which is unfavorable for intermolecular packing and the enhancement of device performance. Second, this strategy reduces the number of halogen modification sites. The current polymerization strategy through end groups replaces one of the chemical modification sites with halogen atoms with a bridging unit when synthesizing PSMA using terminal units and linkers. However, the halogen atoms on terminal groups are crucial as they enhance molecular packings and facilitate charge transfer.[32,33] Additionally, halogen atoms on molecular backbones also play a significant role in tuning the energy levels and light absorption of SMAs and PSMAs.[34–36]

To address the aforementioned issues, we have proposed a new approach to construct PSMAs with grafted SMA units based on the conventional polymerization SMA strategy.[37] PSMAs designed using the grafted SMA strategy feature free end groups

W. Shi, Y. Huang, K. Ma, X. Si, W. Feng, R. Wang, J. Guo, Z. Yao, C. Li, X. Wan, Y. Chen
State Key Laboratory of Elemento-Organic Chemistry
Key Laboratory of Functional Polymer Materials
College of Chemistry
Renewable Energy Conversion and Storage Center (RECAST)
Nankai University
Tianjin 300071, P. R. China
E-mail: lichenxi@nankai.edu.cn; xjwan@nankai.edu.cn

W. Ma, S. Wang
State Key Laboratory for Mechanical Behavior of Materials
Xi'an Jiaotong University
Xi'an 710049, P. R. China
E-mail: msewma@xjtu.edu.cn

A. Clulow, L. Barnsley
Australian Synchrotron
800 Blackburn Road, Clayton, Victoria 3168, Australia

The ORCID identification number(s) for the author(s) of this article can be found under https://doi.org/10.1002/marc.202300407

DOI: 10.1002/marc.202300407

 © 2023 Wiley-VCH GmbH

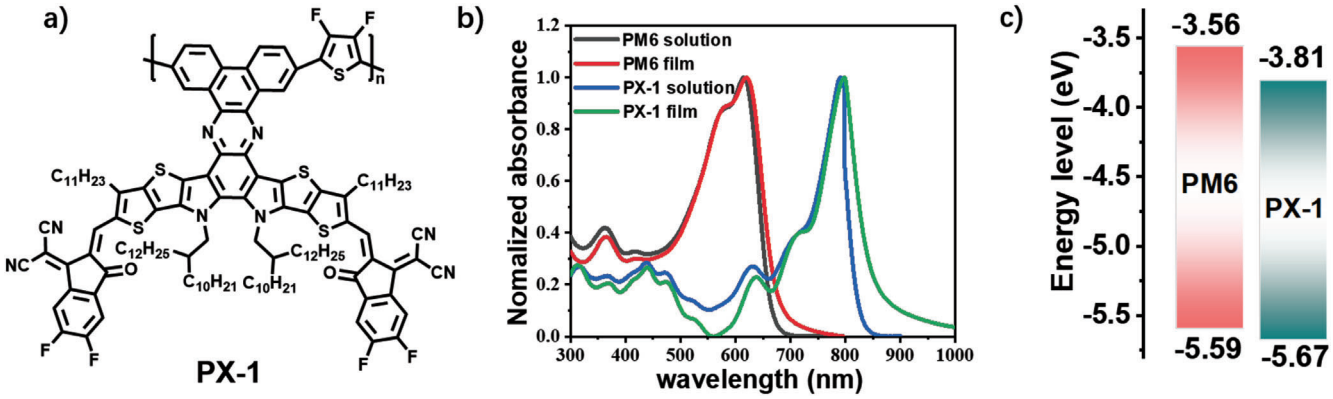

Figure 1. a) Chemical structures of PX-1 b) Absorption spectra of PM6 and PX-1 in CF and in solid films. c) The alignment of energy levels derived from CVs.

that facilitate intermolecular packing, which in turn benefits electron transport. Furthermore, extended conjugation and dual charge transport channels can be formed. Additionally, this design strategy provides more chemical modification sites to create new PSMAs with tunable absorption and energy levels. It is worth noting that the CH acceptors with extended conjugation central cores that we have reported substantially facilitate the above polymerization strategy owing to their versatile chemical functionalization site on the central units and high device performance.[8,38,39] Following this strategy, herein, we have designed and synthesized a polymer acceptor named PX-1 (**Figure 1**a) using the polymerization strategy described above. Utilizing PM6 as the donor polymer, all-PSCs based on PX-1 achieved a promising PCE of 13.55%. This work highlights the potential for achieving higher-efficiency all-PSCs through the careful design of new polymer acceptors using an alternative polymerization pathway.

2. Results and Discussion

2.1. Materials Design and Optical/Electrochemical Properties

The synthetic routes to PX-1 are displayed in Scheme S1 (Supporting Information), and the detailed procedures of synthesis are provided in the Supporting Information. The average molecular weight (M_n) of PX-1 is 13.49 kDa with the polydispersity index (PDI) of 1.57 (Figure S1, Supporting Information). The polymer exhibits good thermal stability with decomposition temperature of 346 °C in the thermogravimetric analyses (Figure S2, Supporting Information). PX-1 has good solubility, which can be easily dissolved in common solvents such as chloroform, chlorobenzene, and toluene.

UV–vis absorption spectra of PX-1 in diluted chloroform solution and neat film are shown in (Figure 1b). PX-1 shows the maximum absorption (λ_{max}) peak located at 792 nm in CF solution. The as-cast solid film of PX-1 displays red-shifted absorption by 8 nm compared with its solution absorption. To further explore the molecular aggregation of the new polymer acceptor, the temperature-dependent UV–vis absorption spectra were measured. The maximum absorption peak of PX-1 was blue-shifted ≈9 nm with increasing temperature from 20 to 100 °C. This should be associated with the strong aggregation of PX-1 (Figure S4, Supporting Information).[40] Cyclic voltammetry (CV) was conducted to investigate the energy levels of the polymer acceptor PX-1. From the onset reduction and oxidation potentials of the CV curves (Figure S3, Supporting Information), the energy levels of PX-1 were estimated. As shown in Figure 1c, the highest occupied molecular orbital (HOMO) level and the lowest unoccupied molecular orbit (LUMO) energy levels of PX-1 are −5.67 and −3.81 eV, respectively, which show well-matched with PM6 (HOMO/LUMO = −5.59/−3.56 eV).

2.2. Photovoltaic Properties

To evaluate the photovoltaic performances of PX-1, we fabricated all-PSCs with an inverted device structure configuration of ITO/ZnO/NMA/PM6: PX-1/MoO_3/Ag (**Figure 2**a). The structure of NMA is shown in Figure S5 (Supporting Information). Owing to the matched energy levels and complementary absorptions with PX-1, PM6 was selected as the donor polymer material. Detailed experimental procedures are presented in the Supporting Information and the detailed device data are listed in Tables S1–S3 (Supporting Information). Optimal current density–voltage (*J*–*V*) curves are illustrated in Figure 2b and the corresponding photovoltaic parameters are listed in **Table 1**. The optimized device of PM6: PX-1 with additive of 2-methoxynaphthalene (2-MN) (100% weight ratio compared to the total mass of PM6:PX-1) showed a promising PCE of 13.55%, which is higher than that the control device with a PCE of 12.36% due to the enhanced short-circuit current density (J_{SC}, from 19.34 to 19.90 mA cm^{-2}) and fill factor (FF, from 66.92 to 71.02%), and nearly remained open-circuit voltage (V_{OC}). The current densities integrated from the external quantum efficiencies (EQE) spectra (Figure 2c) were 18.94 and 18.59 mA cm^{-2} for the device with and without additive, respectively, matching well with the J_{SC} values measured in the *J*–*V* curves. As shown in Figure 2c, the device with the additive of 2-MN shows clearly higher EQE values in the range of 700–800 nm, which is attributed to the improved active layer morphology and facilitated charge transfer/transport process as discussed below.

© 2023 Wiley-VCH GmbH

15213927, 0, Downloaded from https://onlinelibrary.wiley.com/doi/10.1002/marc.202300407 by Nankai University, Wiley Online Library on [25/11/2023]. See the Terms and Conditions (https://onlinelibrary.wiley.com/terms-and-conditions) on Wiley Online Library for rules of use; OA articles are governed by the applicable Creative Commons License

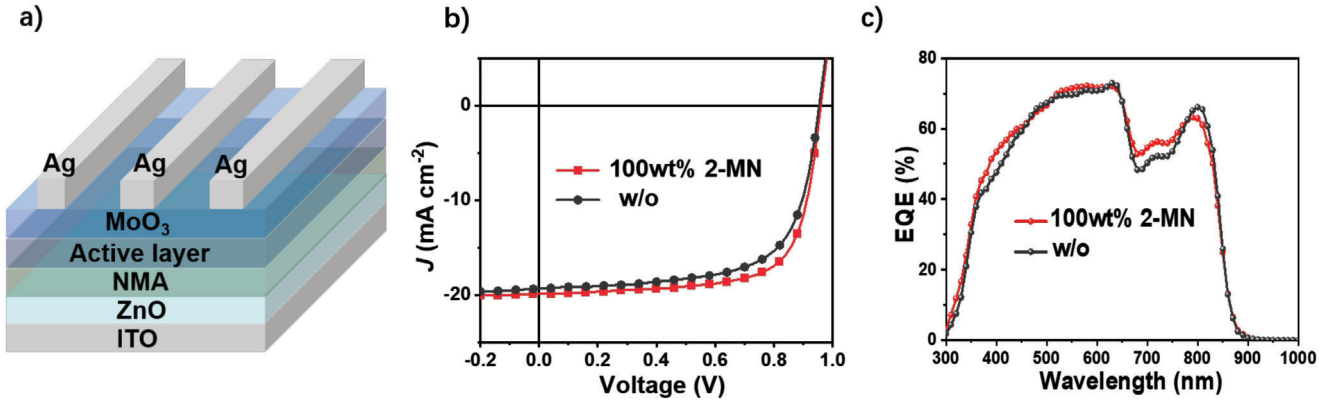

Figure 2. a) Photovoltaic device architecture in this work. b) *J–V* and c) EQE curve of the devices with and without the additive 2-MN.

2.3. Exciton and Carrier Dynamics

The studies on exciton and carrier dynamics were conducted to clarify the variation of photovoltaic parameters of the all-PSCs with and without 2-MN additive. First, we studied the charge recombination process in devices by characterizing the dependence of J_{SC} and V_{OC} under different light intensities. The charge recombination in short-circuit condition is quantified by the power-law dependence of J_{SC} on light intensity. The equation is $J_{SC} \propto P_{light}^{\alpha}$. If α approaches 1, bimolecular recombination is almost negligible, promoting the rapid extraction of charge carriers.[41,42] As displayed in **Figure 3**a, the values of α are almost identical (0.986 and 0.980) with and without 2-MN additive, indicating both devices have less bimolecular recombination. The difference of recombination mechanisms in open-circuit condition can be characterized by the dependence of V_{OC} and the natural logarithm of light intensity. The slope is nKT/q, when n is equal to 2, trap-assisted recombination is dominant, when n is 1, the bimolecular recombination dominates. Among them, K represents the Boltzmann constant, T means thermodynamic temperature, and q is elementary electronic charge.[43] As shown in Figure 3b, the slope values of the PM6: PX-1 device with and without 2-MN are 1.19 and 1.23KT/q, respectively, indicating that there is less trap-assisted recombination in the two devices.

Further, the performance of exciton dissociation and charge collection can be investigated by measuring the correlation of photocurrent density (J_{ph}) and effective voltage (V_{eff}). The result is shown in Figure 3c. We can estimate the exciton dissociation probability (P_{diss}) from the ratio of J_{ph}/J_{sat} under the short-circuit condition. Similarly, the charge extraction efficiency (P_{coll}) can be acquired from the ratio of J_{ph}/J_{sat} under the maximum power output point. The J_{sat} is saturated photocurrent density.[44] As results, the P_{diss} values are 0.94 and 0.93 and the P_{coll} values are 0.78 and 0.72 for the devices with and without 2-MN. The larger P_{diss} and P_{coll} values demonstrated the higher exciton dissociation efficiency and improved charge extraction efficiency for the device with additive of 2-MN, which are attributed to its higher J_{SC} and FF.

Finally, the transient photocurrent (TPC) and transient photovoltage (TPV) tests were used to further explore the carrier dynamics.[45] As plotted in Figure 3d,e, after 2-MN was added to the active layer, the charge extraction time decreased from 0.55 to 0.46 µs, and the photogenerated carrier lifetime increased from 0.25 to 0.43 ms. All the results indicate that charge carrier recombination was suppressed in the device with 2-MN, which is also consistent with the improvement of P_{coll}.

2.4. Morphological Properties

Atomic force microscopy (AFM) and grazing incidence wide-angle X-ray diffraction (GIWAXS) were used to explore the morphology of PM6: PX-1 blend films. As illustrated in AFM height images in **Figure 4**a,b, the two blend films with and without additives all show the small values of the root mean square (RMS) roughness (1.58 and 1.64 nm). As shown in the phase images (Figure 4c,d), the distinct interpenetrating fibril network structures can be observed in the two blend films, especially for the film with 2-MN, which is favorable for charge generation/transport.

The GIWAXS patterns of PM6: PX-1 blend films are displayed in **Figure 5**a,b. The corresponding line-cut profiles are shown in Figure 5c. The neat film of PX-1 shows the edge on dominant orientations (Figure S7, Supporting Information). But when PM6 is added in PX-1 as polymer donor, the two blend films with and without 2-MN all show the clear lamellar stacking peaks in

Table 1. The optimal photovoltaic parameters of PM6: PX-1-based devices with and without 100 wt.% 2-MN under AM 1.5 G Illumination (100 mW cm^{-2}).

Active layer	V_{OC} [V]	J_{SC} [mA cm^{-2}]	J_{SC}^{EQE} [mA cm^{-2}]	FF [%]	PCE [%][a)]
w/o	0.954 (0.959 ± 0.004)	19.34 (19.01 ± 0.27)	18.59	66.92 (67.06 ± 0.73)	12.36 (12.23 ± 0.16)
100 wt.% 2-MN	0.959 (0.958 ± 0.003)	19.90 (19.69 ± 0.27)	18.94	71.02 (70.30 ± 0.70)	13.55 (13.26 ± 0.18)

[a)] Statistical and optimal results are listed in parentheses and outside of parentheses, respectively, and the average parameters were calculated from ten independent cells.

© 2023 Wiley-VCH GmbH

15213927, 0, Downloaded from https://onlinelibrary.wiley.com/doi/10.1002/marc.202300407 by Nankai University, Wiley Online Library on [25/11/2023]. See the Terms and Conditions (https://onlinelibrary.wiley.com/terms-and-conditions) on Wiley Online Library for rules of use; OA articles are governed by the applicable Creative Commons License

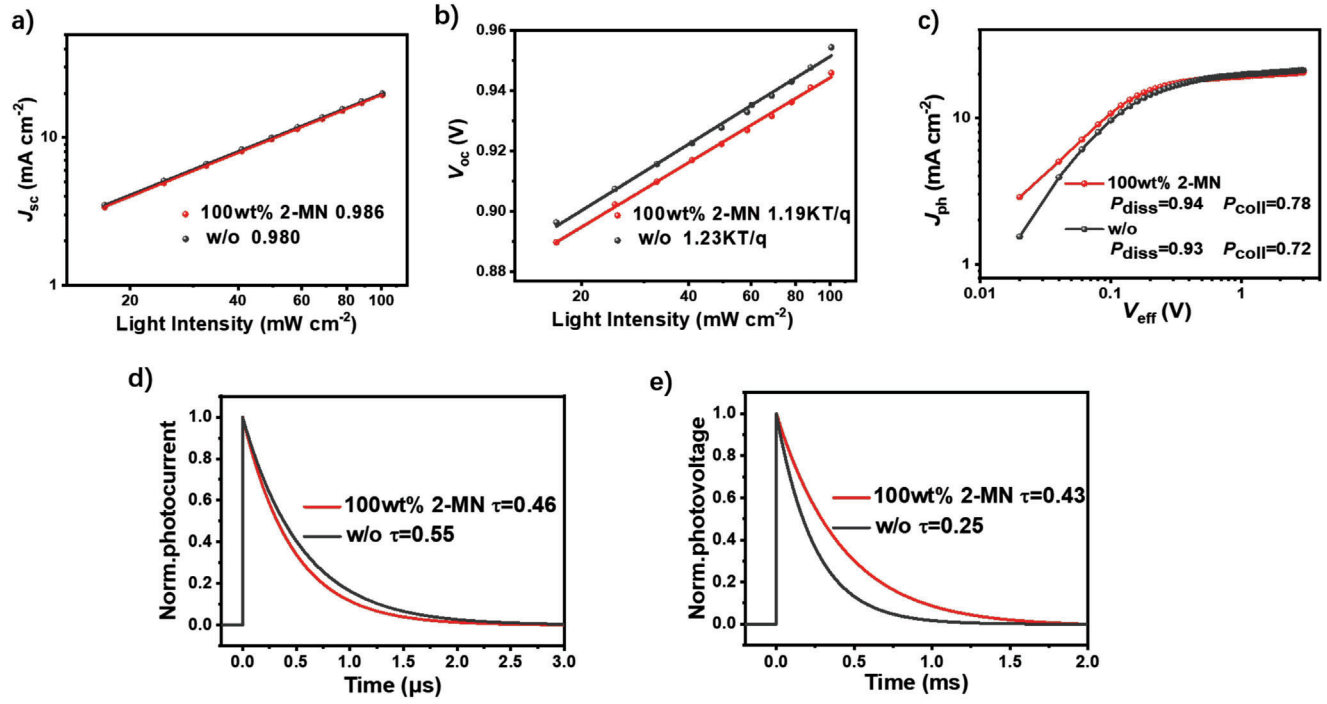

Figure 3. a) light intensity (P) dependence of J_{SC} and b) light intensity (P) dependence of V_{OC}, c) $J_{ph}-V_{eff}$ curves, d) transient photocurrent and e) transient photovoltage measurement of all-PSCs with and without 100 wt.% 2-MN.

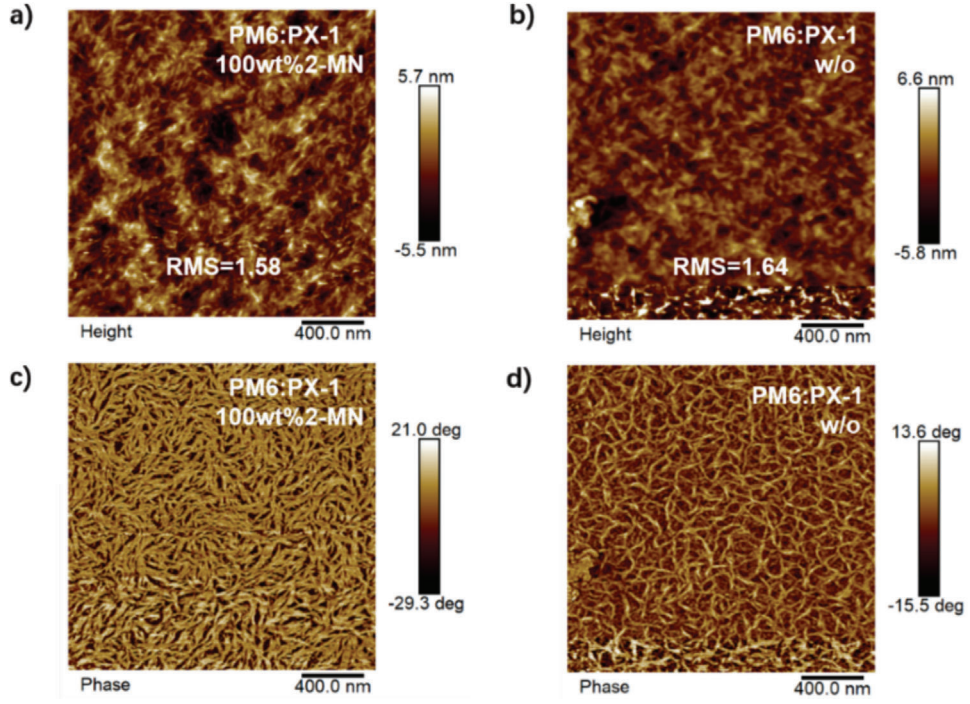

Figure 4. AFM height images of PM6: PX-1 blends a) with and b) without 100 wt.% 2-MN. AFM phase images of PM6: PX-1 blends c) with and d) without 100 wt.% 2-MN.

© 2023 Wiley-VCH GmbH

15213927, 0, Downloaded from https://onlinelibrary.wiley.com/doi/10.1002/marc.202300407 by Nankai University, Wiley Online Library on [25/11/2023]. See the Terms and Conditions (https://onlinelibrary.wiley.com/terms-and-conditions) on Wiley Online Library for rules of use; OA articles are governed by the applicable Creative Commons License

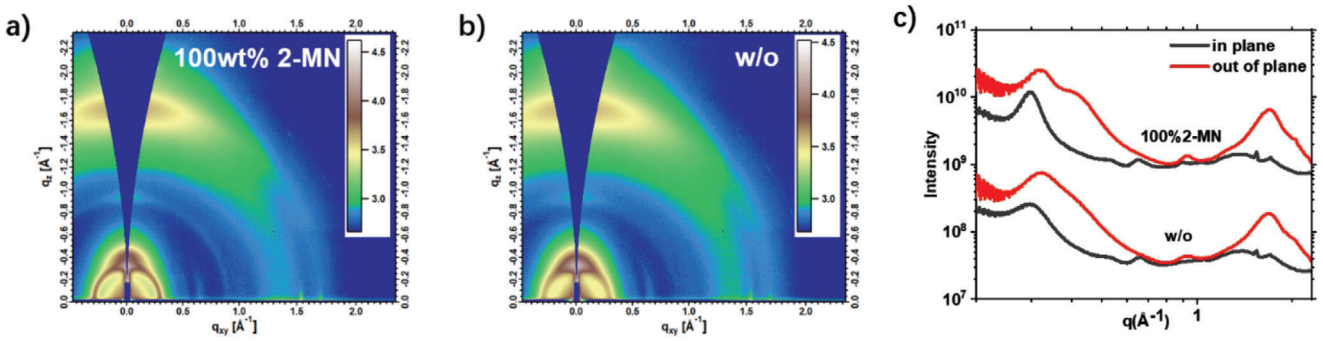

Figure 5. 2D GIWAXS images of PM6: PX-1 blends a) with and b) without 100 wt.% 2-MN. c) 1D GIWAXS profiles of PM6: PX-1 blends with and without 100 wt.% 2-MN.

Table 2. The detailed parameters of energy losses for optimized OSCs.

Active Layer	E_g^{pv} [eV]	V_{OC}^{SQ} [V]	ΔE_1 [eV]	ΔE_2 [eV]	ΔE_3 [eV]	EQE_{EL} [E^{-2}]	V_{OC} [V]	E_{loss} [eV]
2-MN	1.480	1.210	0.270	0.063	0.188	0.07	0.959	0.521
w/o	1.480	1.210	0.270	0.060	0.196	0.05	0.954	0.526

the out-of-plane direction, which indicates the face-on dominant orientations and ordered stacking in blend films. Besides, the similar $\pi-\pi$ distance (3.73 Å/3.74 Å) (Table S4, Supporting Information) and the slightly enhanced $\pi-\pi$ stacking coherence length (Table S5, Supporting Information) can be observed for the blend film with 2-MN (18.85 Å) compared with that of the blend film without 2-MN (18.18 Å).[46] The ordered molecular packing behaviors of the all-polymer active layers are consistent with AFM results, which can facilitate the efficient exciton dissociation and charge transport in the photovoltaic device.[47]

2.5. Energy Loss Analysis

In order to understand the reason for high V_{OC} of PM6: PX-1-based all-PSCs, a detailed energy loss analysis was conducted. The E_{loss} of the devices with and without additive 2-MN were calculated to be 0.521 and 0.526 V following the equation $E_{loss} = E_g - qV_{OC}$.[48] The E_g of the blend films was estimated from the intersection of normalized optical absorption and PL curves (Figure S8a, Supporting Information). Then, based on the Shockley–Queisser (SQ) theory,[49] the E_{loss} can be divided into three parts: $E_{loss} = \Delta E_1 + \Delta E_2 + \Delta E_3$ (ΔE_1 is the radiative recombination loss above the bandgap, ΔE_2 is the radiative recombination loss below the bandgap, ΔE_3 is the non-radiative energy loss). As shown in **Table 2**, the ΔE_1 was calculated from the equation: $\Delta E_1 = E_g - qV_{OC}^{SQ}$[50]. The values of ΔE_1 of PM6: PX-1-based devices with and without 2-MN are identical due to their same E_g and V_{OC}^{SQ}. The second part (ΔE_2) of the PM6:PX-1-based device with 2-MN was calculated to be 0.063 eV, which is slightly larger than that of the PM6:PX-1-based device without additvie (0.060 eV). The ΔE_3 is calculated by using the equation of $\Delta E_3 = -kT\ln(EQE_{EL})$.[51] The PM6:PX-1-based device with 2-MN shows a higher EQE_{EL} of 7×10^{-4} compared to the device without additive with the EQE_{EL} of 5×10^{-4} (Figure S8b, Supporting Information). The corresponding ΔE_3 were estimated to be 0.188 and 0.196 eV for the PM6:PX-1-based devices with and without additives, respectively. It is worthy to note that the PM6: PX-1-based all-PSCs, especially the device with additive, exhibit low ΔE_3 with values below 0.2 eV, which are smaller than most of the state-of-the-art devices.[52] Considering the large ΔE_3 is one of the main E_{loss} for OSCs, the above results demonstrate much potential of this type of polymer acceptor for achieving higher efficiency devices.

3. Conclusion

In conclusion, we successfully designed and synthesized a polymer acceptor, named PX-1, through an alternative polymerization strategy different from the conventional polymerization SMA strategy for polymer acceptors, i.e., polymerization between the central building blocks of SMAs with linkers. This approach can free the end groups of A-D-A type small molecule monomers and hold great potential for achieving higher efficiency PSMAs through careful regulation of both monomer and linker groups. The all-PSC based on PM6:PX-1 demonstrated a promising PCE of 13.55%. We believe that by employing the aforementioned strategy and careful monomer design, it is possible to design polymer acceptors with higher efficiency in the future.

4. Experimental Section

Experimental methods are available in the Supporting Information.

Supporting Information

Supporting Information is available from the Wiley Online Library or from the author.

Acknowledgements

The authors gratefully acknowledge the financial support from NSFC (52025033 and 21935007) MoST of China (2022YFB4200400 and

© 2023 Wiley-VCH GmbH

15213927, 0, Downloaded from https://onlinelibrary.wiley.com/doi/10.1002/marc.202300407 by Nankai University, Wiley Online Library on [25/11/2023]. See the Terms and Conditions (https://onlinelibrary.wiley.com/terms-and-conditions) on Wiley Online Library for rules of use; OA articles are governed by the applicable Creative Commons License

2019YFA0705900). The X-ray data of this research was undertaken on the SAXS/WAXS beamline at the Australian Synchrotron, part of ANSTO. The authors thank Dr. Nigel Kirby and Dr. Susanne Seibt for assistance with data acquisition.

Conflict of Interest

The authors declare no conflict of interest.

Data Availability Statement

The data that support the findings of this study are available in the supplementary material of this article.

Keywords

all-polymer solar cells, polymer acceptors, polymerization

Received: July 5, 2023
Revised: August 27, 2023
Published online:

[1] A. Mishra, P. Bauerle, *Angew Chem., Int. Ed.* **2012**, *51*, 2020.
[2] Y. N. Sun, M. J. Chang, L. X. Meng, X. J. Wan, H. H. Gao, Y. M. Zhang, K. Zhao, Z. H. Sun, C. X. Li, S. R. Liu, H. K. Wang, J. J. Liang, Y. S. Chen, *Nat. Electron.* **2019**, *2*, 513.
[3] J. Zhang, H. S. Tan, X. Guo, A. Facchetti, H. Yan, *Nat. Energy* **2018**, *3*, 720.
[4] J. Yuan, Y. Zhang, L. Zhou, G. Zhang, H.-L. Yip, T.-K. Lau, X. Lu, C. Zhu, H. Peng, P. A. Johnson, M. Leclerc, Y. Cao, J. Ulanski, Y. Li, Y. Zou, *Joule* **2019**, *3*, 1140.
[5] L. Ye, K. Weng, J. Xu, X. Du, S. Chandrabose, K. Chen, J. Zhou, G. Han, S. Tan, Z. Xie, Y. Yi, N. Li, F. Liu, J. M. Hodgkiss, C. J. Brabec, Y. Sun, *Nat. Commun.* **2020**, *11*, 6005.
[6] L. Meng, Y. Zhang, X. Wan, C. Li, X. Zhang, Y. Wang, X. Ke, Z. Xiao, L. Ding, R. Xia, H.-L. Yip, Y. Cao, Y. Chen, *Science* **2018**, *361*, 1094.
[7] L. Xie, W. Song, J. Ge, B. Tang, X. Zhang, T. Wu, Z. Ge, *Nano Energy* **2021**, *82*, 105770.
[8] H. Chen, Y. Zou, H. Liang, T. He, X. Xu, Y. Zhang, Z. Ma, J. Wang, M. Zhang, Q. Li, C. Li, G. Long, X. Wan, Z. Yao, Y. Chen, *Sci. China :Chem.* **2022**, *65*, 1362.
[9] L. Zhan, S. Li, X. Xia, Y. Li, X. Lu, L. Zuo, M. Shi, H. Chen, *Adv. Mater.* **2021**, *31*, 2007231.
[10] C. Li, J. Zhou, J. Song, J. Xu, H. Zhang, X. Zhang, J. Guo, L. Zhu, D. Wei, G. Han, J. Min, Y. Zhang, Z. Xie, Y. Yi, H. Yan, F. Gao, F. Liu, Y. Sun, *Nat. Energy* **2021**, *6*, 605.
[11] L. Zhu, M. Zhang, J. Xu, C. Li, J. Yan, G. Zhou, W. Zhong, T. Hao, J. Song, X. Xue, Z. Zhou, R. Zeng, H. Zhu, C.-C. Chen, R. C. I. MacKenzie, Y. Zou, J. Nelson, Y. Zhang, Y. Sun, F. Liu, *Nat. Mater.* **2022**, *21*, 656.
[12] Z. Chen, H. Yao, J. Wang, J. Zhang, T. Zhang, Z. Li, J. Qiao, S. Xiu, X. Hao, J. Hou, *Energy Environ. Sci.* **2023**, *16*, 2637.
[13] T. Chen, S. Li, Y. Li, Z. Chen, H. Wu, Y. Lin, Y. Gao, M. Wang, G. Ding, J. Min, Z. Ma, H. Zhu, L. Zuo, H. Chen, *Adv. Mater.* **2023**, *35*, 2300400.
[14] W. Gao, F. Qi, Z. Peng, F. R. Lin, K. Jiang, C. Zhong, W. Kaminsky, Z. Guan, C.-S. Lee, T. J. Marks, H. Ade, A. K. Y. Jen, *Adv. Mater.* **2022**, *34*, 2202089.
[15] Y. Wei, Z. Chen, G. Lu, N. Yu, C. Li, J. Gao, X. Gu, X. Hao, G. Lu, Z. Tang, J. Zhang, Z. Wei, X. Zhang, H. Huang, *Adv. Mater.* **2022**, *34*, 2204718.
[16] G. Wang, F. S. Melkonyan, A. Facchetti, T. J. Marks, *Angew. Chem., Int. Ed.* **2019**, *58*, 4129.
[17] Z.-G. Zhang, Y. Yang, J. Yao, L. Xue, S. Chen, X. Li, W. Morrison, C. Yang, Y. Li, *Angew. Chem., Int. Ed.* **2017**, *56*, 13503.
[18] H. Yu, Y. Wang, H. K. Kim, X. Wu, Y. Li, Z. Yao, M. Pan, X. Zou, J. Zhang, S. Chen, D. Zhao, F. Huang, X. Lu, Z. Zhu, H. Yan, *Adv. Mater.* **2022**, *34*, 2200361.
[19] L. Zhixiang, Z. Zhe, C. Hongbin, Z. Yunxin, Y. Yuan-Qiu-Qiang, L. Ziqi, Z. Bin, L. Miaomiao, L. Chenxi, Y. Zhaoyang, W. Xiangjian, K. Bin, C. Yongsheng, *Adv. Energy Mater.* **2023**, *23*, 2300301.
[20] Z. Ge, J. Qiao, Y. Li, J. Song, C. Zhang, Z. Fu, M. H. Jee, X. Hao, H. Y. Woo, Y. Sun, *Adv. Mater.* **2023**, *35*, 2301906.
[21] T. Zhang, Y. Xu, H. Yao, J. Zhang, P. Bi, Z. Chen, J. Wang, Y. Cui, L. Ma, K. Xian, Z. Li, X. Hao, Z. Wei, J. Hou, *Energy Environ. Sci.* **2023**, *16*, 1581.
[22] Y. Cai, C. Xie, Q. Li, C. Liu, J. Gao, M. H. Jee, J. Qiao, Y. Li, J. Song, X. Hao, H. Y. Woo, Z. Tang, Y. Zhou, C. Zhang, H. Huang, Y. Sun, *Adv. Mater.* **2023**, *35*, 2208165.
[23] J. Guo, X. Xia, B. Qiu, J. Zhang, S. Qin, X. Li, W. Lai, X. Lu, L. Meng, Z. Zhang, Y. Li, *Adv. Mater.* **2023**, *35*, 2211296.
[24] Z.-G. Zhang, Y. Li, *Angew. Chem., Int. Ed.* **2021**, *60*, 4422.
[25] Z. Luo, T. Liu, R. Ma, Y. Xiao, L. Zhan, G. Zhang, H. Sun, F. Ni, G. Chai, J. Wang, C. Zhong, Y. Zou, X. Guo, X. Lu, H. Chen, H. Yan, C. Yang, *Adv. Mater.* **2020**, *32*, 2005942.
[26] M. Kataria, H. D. Chau, N. Y. Kwon, S. H. Park, M. J. Cho, D. H. Choi, *ACS Energy Lett.* **2022**, *7*, 3835.
[27] K. Ma, H. Liang, Y. Wang, Z. Xiao, C. Jiang, W. Feng, Z. Zhang, X. Si, J. Liu, X. Wan, B. Kan, C. Li, Z. Yao, Y. Chen, *ACS Mater. Lett.* **2023**, *5*, 884.
[28] W. Zhu, A. P. Spencer, S. Mukherjee, J. M. Alzola, V. K. Sangwan, S. H. Amsterdam, S. M. Swick, L. O. Jones, M. C. Heiber, A. A. Herzing, G. Li, C. L. Stern, D. M. DeLongchamp, K. L. Kohlstedt, M. C. Hersam, G. C. Schatz, M. R. Wasielewski, L. X. Chen, A. Facchetti, T. J. Marks, *J. Am. Chem. Soc.* **2020**, *142*, 14532.
[29] B. Fan, W. Gao, R. Zhang, W. Kaminsky, F. R. Lin, X. Xia, Q. Fan, Y. Li, Y. An, Y. Wu, M. Liu, X. Lu, W. J. Li, H.-L. Yip, F. Gao, A. K. Y. Jen, *J. Am. Chem. Soc.* **2023**, *145*, 5909.
[30] G. Sun, X. Jiang, X. Li, L. Meng, J. Zhang, S. Qin, X. Kong, J. Li, J. Xin, W. Ma, Y. Li, *Nat. Commun.* **2022**, *13*, 5267.
[31] J. Zhang, C. H. Tan, K. Zhang, T. Jia, Y. Cui, W. Deng, X. Liao, H. Wu, Q. Xu, F. Huang, Y. Cao, *Adv. Energy Mater.* **2021**, *11*, 2102559.
[32] H. Wang, H. Chen, W. Xie, H. Lai, T. Zhao, Y. Zhu, L. Chen, C. Ke, N. Zheng, F. He, *Adv. Funct. Mater.* **2021**, *31*, 2100877.
[33] T. Zhao, C. Cao, H. Wang, X. Shen, H. Lai, Y. Zhu, H. Chen, L. Han, T. Rehman, F. He, *Macromolecules* **2021**, *54*, 11468.
[34] L. Yan, H. Zhang, Q. An, M. Jiang, A. Mahmood, M. H. Jee, H.-R. Bai, H.-F. Zhi, S. Zhang, H. Y. Woo, J.-L. Wang, *Angew. Chem., Int. Ed.* **2022**, *61*, e202209454.
[35] H. Yu, Z. Qi, J. Yu, Y. Xiao, R. Sun, Z. Luo, A. M. H. Cheung, J. Zhang, H. Sun, W. Zhou, S. Chen, X. Guo, X. Lu, F. Gao, J. Min, H. Yan, *Adv. Energy Mater.* **2021**, *11*, 2003171.
[36] R. Sun, W. Wang, H. Yu, Z. Chen, X. Xia, H. Shen, J. Guo, M. Shi, Y. Zheng, Y. Wu, W. Yang, T. Wang, Q. Wu, Y. Yang, X. Lu, J. Xia, C. J. Brabec, H. Yan, Y. Li, J. Min, *Joule* **2021**, *5*, 1548.
[37] Y.-Z. Huang, X. Si, R. Wang, K. Ma, W. Shi, C. Jiang, Y. Lu, C. Li, X. Wan, Y. Chen, *J. Mater. Chem. A* **2023**, *11*, 14768.
[38] H. Chen, H. Liang, Z. Guo, Y. Zhu, Z. Zhang, Z. Li, X. Cao, H. Wang, W. Feng, Y. Zou, L. Meng, X. Xu, B. Kan, C. Li, Z. Yao, X. Wan, Z. Ma, Y. Chen, *Angew. Chem., Int. Ed.* **2022**, *61*, e202209580.
[39] Y. Zou, H. Chen, X. Bi, X. Xu, H. Wang, M. Lin, Z. Ma, M. Zhang, C. Li, X. Wan, G. Long, Y. Zhaoyang, Y. Chen, *Energy Environ. Sci.* **2022**, *15*, 3519.
[40] J. Du, K. Hu, J. Zhang, L. Meng, J. Yue, I. Angunawela, H. Yan, S. Qin, X. Kong, Z. Zhang, B. Guan, H. Ade, Y. Li, *Nat. Commun.* **2021**, *12*, 5264.

 © 2023 Wiley-VCH GmbH

15213927, 0, Downloaded from https://onlinelibrary.wiley.com/doi/10.1002/marc.202300407 by Nankai University, Wiley Online Library on [25/11/2023]. See the Terms and Conditions (https://onlinelibrary.wiley.com/terms-and-conditions) on Wiley Online Library for rules of use; OA articles are governed by the applicable Creative Commons License

[41] D. Credgington, F. C. Jamieson, B. Walker, T.-Q. Nguyen, J. R. Durrant, *Adv. Mater.* **2012**, *24*, 2135.
[42] A. K. K. Kyaw, D. H. Wang, C. Luo, Y. Cao, T.-Q. Nguyen, G. C. Bazan, A. J. Heeger, *Adv. Energy Mater.* **2014**, *4*, 1301469.
[43] Q. Chen, H. Huang, D. Hu, C. e. Zhang, X. Xu, H. Lu, Y. Wu, C. Yang, Z. Bo, *Adv. Mater.* **2023**, *35*, 2211372.
[44] N. Gasparini, M. Salvador, S. Strohm, T. Heumueller, I. Levchuk, A. Wadsworth, J. H. Bannock, J. C. de Mello, H.-J. Egelhaaf, D. Baran, I. McCulloch, C. J. Brabec, *Adv. Energy Mater.* **2017**, *7*, 1700770.
[45] I. Riedel, J. Parisi, V. Dyakonov, L. Lutsen, D. Vanderzande, J. C. Hummelen, *Adv. Funct. Mater.* **2004**, *14*, 38.
[46] H. Alexander, B. Wim, G. James, S. Eric, G. Eliot, K. Rick, M. Alastair, C. Matthew, R. Bruce, P. Howard, *J. Phys.: Conf. Ser.* **2010**, *247*, 012007.
[47] T. Liu, Y. Zhang, Y. Shao, R. Ma, Z. Luo, Y. Xiao, T. Yang, X. Lu, Z. Yuan, H. Yan, Y. Chen, Y. Li, *Adv. Funct. Mater.* **2020**, *30*, 2000456.
[48] K. Vandewal, J. Benduhn, V. C. Nikolis, *Sustainable Energy Fuels* **2018**, *2*, 538.
[49] U. Rau, B. Blank, T. C. M. Müller, T. Kirchartz, *Phys. Rev. Appl.* **2017**, *7*, 044016.
[50] Y. Wang, D. Qian, Y. Cui, H. Zhang, J. Hou, K. Vandewal, T. Kirchartz, F. Gao, *Adv. Energy Mater.* **2018**, *8*, 1801352.
[51] X.-K. Chen, D. Qian, Y. Wang, T. Kirchartz, W. Tress, H. Yao, J. Yuan, M. Hülsbeck, M. Zhang, Y. Zou, Y. Sun, Y. Li, J. Hou, O. Inganäs, V. Coropceanu, J.-L. Bredas, F. Gao, *Nat. Energy* **2021**, *6*, 799.
[52] Y. Shi, Y. Chang, K. Lu, Z. Chen, J. Zhang, Y. Yan, D. Qiu, Y. Liu, M. A. Adil, W. Ma, X. Hao, L. Zhu, Z. Wei, *Nat. Commun.* **2022**, *13*, 3256.

© 2023 Wiley-VCH GmbH

15213927, 0, Downloaded from https://onlinelibrary.wiley.com/doi/10.1002/marc.202300407 by Nankai University, Wiley Online Library on [25/11/2023]. See the Terms and Conditions (https://onlinelibrary.wiley.com/terms-and-conditions) on Wiley Online Library for rules of use; OA articles are governed by the applicable Creative Commons License